# Measurement of Cosmic Ray and Trapped Proton LET Spectra on the STS-95 HOST Mission

E. G. Stassinopoulos, J. L. Barth, *Fellow, IEEE,* C. A. Stauffer

***Abstract*— This paper reports on *in situ* measurements of the Linear-Energy-Transfer (LET) spectra of galactic cosmic rays and their progeny and of trapped Van Allen belt protons as recorded by a Pulse Height Analyzer (PHA) radiation spectrometer which flew on the STS-95 DISCOVERY mission on the Hubble Orbital Systems Test (HOST) cradle. The Shuttle was launched on 29 October 1998 and had a mission duration of 8.5 days during the minimum phase of the solar activity cycle. The orbit of the STS-95 was about 550 km altitude and 28.5° inclination. Close agreement was seen between radiation environment model predictions and the measurements of the PHA. Agreement is obtained by considering the directionality of the radiation interacting with the Shuttle structure.**

***Index Terms*—cosmic rays, pulse height analyzer, space radiation, spectrometer, trapped protons**

## I. INTRODUCTION

THIS paper presents the results of the measurements of a Pulse Height Analyzer (PHA) radiation spectrometer which was flown on the STS-95 DISCOVERY mission. The purpose is to expand the analysis that was presented previously [1] to include calculations with the new AP9 mean trapped proton model [2] and to investigate the reason for differences between observed and expected PHA measurements. The PHA spectrometer [3] is a low power, small size, and lightweight instrument consisting of a detector that is based on arrays of silicon p-n junctions in the form of a 256 kbit Static Random Access Memory (SRAM). The detector measures the energy deposited in the microelectronic device by: (a) cosmic rays, (b) energetic protons via their nuclear interactions in the sensitive volumes and immediate surrounding materials, and (c) by their secondary daughter products. The PHA spectrometer is a pedigreed, space-qualified instrument with a Technology Readiness Level of 9 (TRL-9). The use of p-n junction arrays in microelectronic memory devices, operating as detectors of deposited energy, is a main feature of this spectrometer. It operates on well-known principles of processing pulse height data. [1]

Paper submitted for review on October 12, 2016

E. G. Stassinopoulos is with the National Aeronautics and Space Administration located at Goddard Space Flight Center, Greenbelt, MD 20771 USA (e-mail: egstassinop@verizon.net).

J. L. Barth is with the National Aeronautics and Space Administration located at Goddard Space Flight Center, Greenbelt, MD 20771 USA (e-mail: jbarth@ieee.org).

C. A. Stauffer is with AS and D Inc. at the National Aeronautics and Space Administration located at Goddard Space Flight Center, Greenbelt, MD 20771 USA (e-mail: craig.a.stauffer@nasa.gov).

## II. SPECTROMETER DESIGN

The unique feature of the spectrometer design is the 32kx8 SRAM based detector with all of its bits connected in parallel and unbiased. This SRAM was selected because it is similar in feature size to other components being used when the PHA was designed in the 1990s. It primarily consists of a large area of identical transistors making up each bit in the 256 kbit SRAM memory array. An intrinsic voltage of the junctions, about 1 V, exists within the device. The SRAM has a die area of 0.25 $cm^2$, a node (junction) cross section of 4 $\mu m^2$, a sensitive volume depth of 14 μm, and an EPItaxial (EPI) layer of 5 μm. The spectrometer circuit board weight is 0.5 pounds, and its power requirement is 0.25 watt. The Linear Energy Transfer (LET) application range of the PHA spectrometer is specified as 1.12 to 16.1 MeV-$cm^2$/mg.

A particle incident on any of the cells generates a charge in a p-n junction, which is collected by the preamp. Simultaneous events in two or more cells within 3 microseconds are treated as one event (additive). The resultant pulse is subsequently amplified and digitized and is sorted by the device's electronics, relative to its amplitude, into one of the 12 to 127 discrete channels in a memory component. The dead time of the PHA spectrometer is about 2.3 milliseconds, and the PHA is limited to an event rate of 435 counts per second. The PHA spectrometer is designed for space and aviation applications [4,5]. [1]

## III. THE HOST PHA SPECTROMETER

The PHA spectrometer was mounted on the top of the Hubble Orbital Systems Test (HOST) cradle in the cargo bay of the STS-95 DISCOVERY Shuttle. It was suspended on the uppermost truss of the cradle. Fig. 1 is a photo of the Shuttle on its side with the cargo bay doors open, and it indicates the position of the HOST cradle where the PHA experiment was mounted. The photo shows that the PHA was located above the Shuttle vehicle and the bulk of the payload. In this

configuration, the shielding geometry that prevailed was simply a 2π exposure, since the backside of the instrument was heavily shielded by the bulk of the Shuttle and the other payloads behind the PHA. This configuration allowed the detector to be accessible to predominately normally incident particles.

The instrument package was constructed with a hole in the cover directly above the SRAM detector facing out into space with only the ~0.2 g/cm$^2$ Kovar detector lid as shielding (10 mils Kovar = 29 mils equivalent aluminum). Fig. 2 is a photo of the instrument with its cover removed. [1]

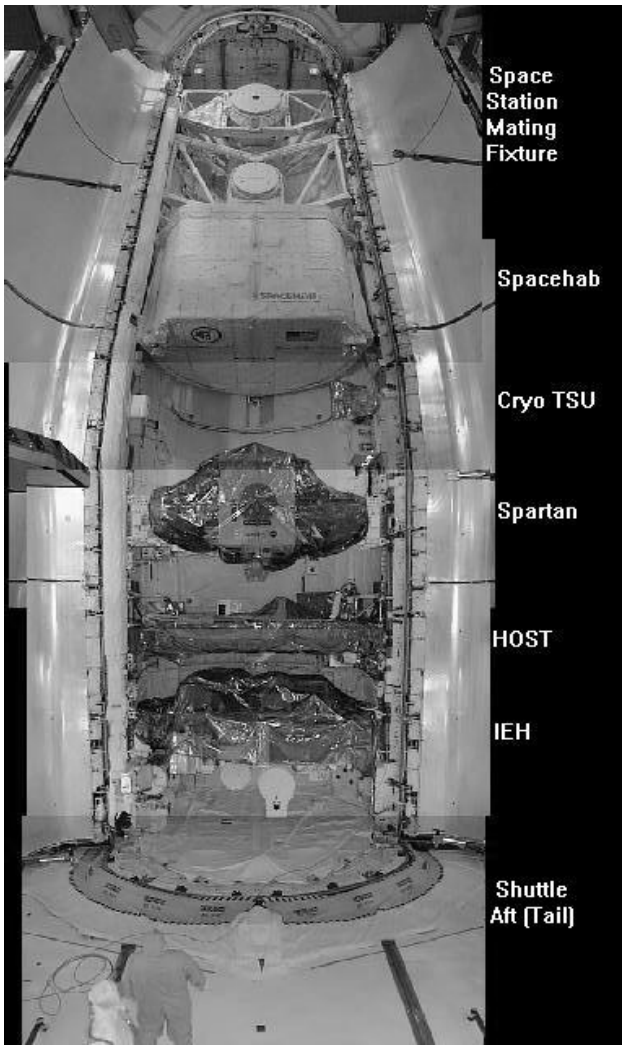

Fig. 1. STS-95 on its side, cargo door open

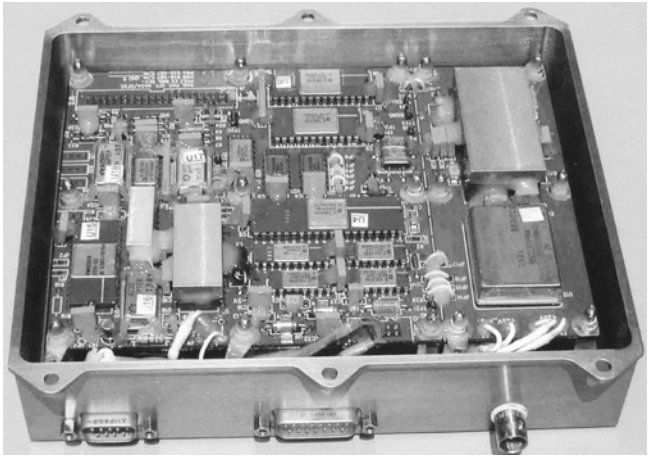
Fig. 2. Photo of the PHA spectrometer instrument with cover removed [1]

## IV. Spectrometer Calibration

Calibration of the PHA for sensitivity to heavy ion particles was accomplished at the Van de Graaff facility of the Brookhaven National Laboratory in Upton, New York. Five ion species were used as listed in Table 1, which also shows the energies, the corresponding LETs, and the penetration ranges of these particles impinging on the surface of the detector before they passed through the 5 μm EPI layer. Fig. 3 shows the LET versus channel-number calibration curve for C-12, O-16, Mg-24, Si-28, and Cl-35 heavy ion particles.

The data were fit to a curve with an exponential function that was used to identify LET values for events occurring in specific channels and to define the instrument's LET range of application as 1.12 to 16.1 MeV-cm$^2$/mg. This range corresponds to channel numbers 12 to 127. The channels below number 12 were not usable due to electromagnetic interference (EMI) from other systems on the spacecraft, especially from motors. This induced noise on the power and ground lines propagated through the EMI filters and into the PHA electronics simulating a PHA event in the low channels. Channel 127 integrated all particles with LETs greater than 16.1 MeV-cm$^2$/mg. All calibration exposures were performed at normal incidence with the detector unbiased.

TABLE 1
BROOKHAVEN CALIBRATION BEAMS: IONS, ENERGIES, LET'S, RANGE

| Z | Ion | Energy (MeV/n) | Ion LET (MeV•cm$^2$/mg) | Range (Si) (μm) |
|---|---|---|---|---|
| 6 | $C^{12}$ | 8.30 | 1.46 | 180.43 |
| 8 | $O^{16}$ | 8.00 | 2.61 | 137.78 |
| 12 | $Mg^{24}$ | 6.71 | 6.01 | 84.16 |
| 14 | $Si^{28}$ | 6.66 | 7.81 | 77.16 |
| 17 | $Cl^{35}$ | 6.06 | 11.50 | 64.41 |

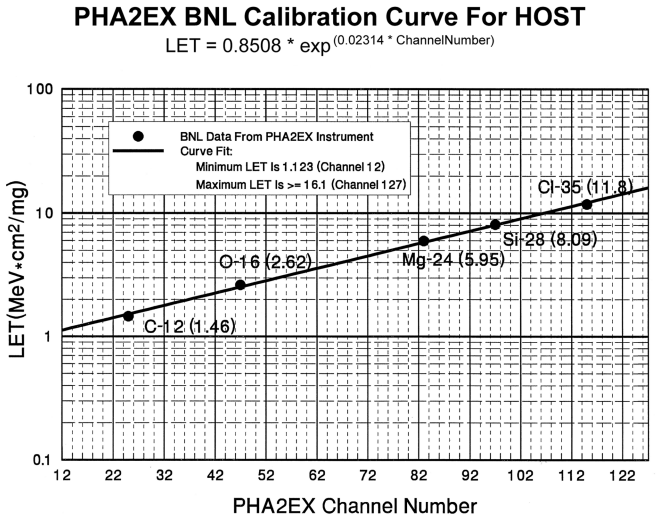


Fig. 3. Heavy Ion Calibration Curve for PHA, LET=0.8508 • exp (0.02314 , Channel Number) [1]

The detector's proton sensitivity was determined at the University of Indiana Cyclotron facility in Bloomington, Indiana. Irradiations were performed with three proton energies: 58.7, 110.0, and 192.7 MeV. The average normalized proton fluence versus proton energy per calibration event is plotted in Fig. 4 where an exponential curve is fitted through the data points. The response of the detector is exponential rather than linear, because we are using an unbiased SRAM as the detector rather than a typical silicon detector reversed-biased PN junction (diode) with a large surface area. As indicated in the calibration tests, it takes about $1.75 \times 10^5$ protons with energies of 59 MeV to generate a recordable pulse in the instrument, but only $6.2 \times 10^4$ protons with energies of 193 MeV to produce an event. [1]

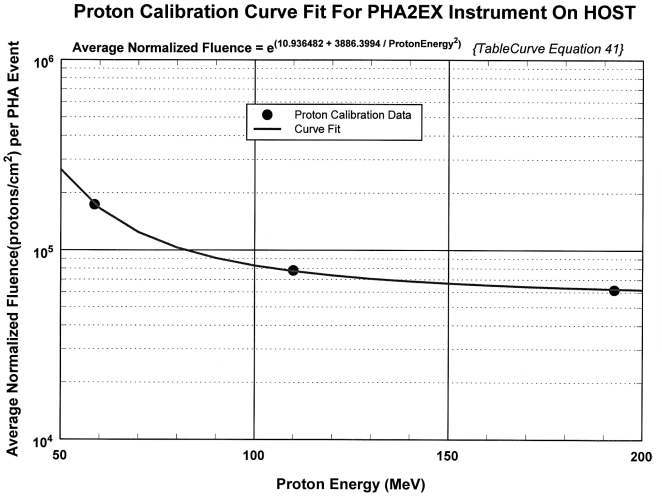


Fig. 4. Energetic proton calibration curve for PHA [1]

## V. HOST PHA Spectrometer Measurements and Rate Predictions

### *A. Trapped Proton and Galactic Cosmic Ray Exposure of the STS-95 Orbit*

The orbit of the STS-95 Mission was about 550 km altitude and 28.5° inclination. In this orbit, the Shuttle traversed regions inside and outside of the South Atlantic Anomaly (SAA) spending approximately 10% of the time in the SAA. The orbit takes about 95 minutes per revolution, and the spacecraft performs approximately 15 revolutions per day. Depending on the altitude of the Shuttle orbit and the environment model used for predictions, 8-12 orbits traverse the SAA daily where it is exposed to energetic trapped protons. The STS-95 traversals through the SAA were of limited duration, i.e. from about 2 minutes for just grazing passes to about 26 minutes for passes through its center.

Solar and galactic cosmic rays cannot be trapped in the Van Allen Belts. However at higher inclinations where the Earth's magnetic field is weaker, the Shuttle is exposed to particles of solar and galactic origin. Fig. 5 illustrates an approximation of Earth's magnetic attenuation of heavier ions where the relationship between the dipole shell parameter, L, and cutoff rigidity is used to determine the particle energy required to penetrate the magnetosphere. The globe's magnetic field is effectively shielding the SAA from the lower energy particles by deflecting them, meaning that protons up to about 2.9 GeV and heavier ions up to about 1.15 GeV/n are prevented from penetrating into the inner zone of the Van Allen Belts in a process that involves the ratio of their momentum-over-charge, i.e. the magnetic rigidity concept. Higher energy protons and cosmic rays can penetrate the SAA, but only as transiting particles. For galactic cosmic rays, it is assumed that they arrive fully ionized in the vicinity of the Earth, and their intensity varies with the solar activity cycle by a factor of about two with lower abundances during solar maximum and higher during solar minimum.

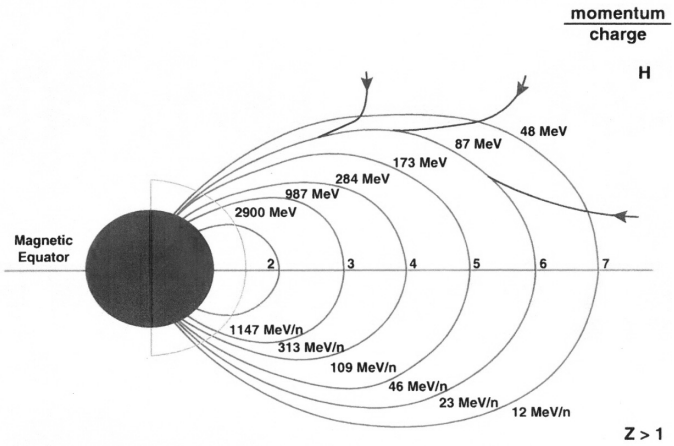


Fig. 5. Energy of cosmic ray ions, required to penetrate regions of the magnetosphere. Units for the top half are rigidity MV. z/A for the bottom half (heavier ions) is approximated with a constant value of 0.5.

### *B. Location and Rates of Measured Events*

All measured events were grouped into two data sets: 1) events inside the SAA, mostly produced by energetic protons along with possible rare contributions from penetrating

(transiting) cosmic rays and 2) events observed outside of the SAA, caused by heavy ion cosmic rays. In the Sections below, the location of the measured events is described and comparisons of measured and predicted rates are provided.

*1) Trapped Proton Induced Events*

During the 8.5 days of the HOST mission duration, STS-95 experienced 59 SAA traversals. The flight paths intersecting this region varied from just grazing the SAA to deeply penetrating into the higher intensity trapped proton domain. About half of the 59 traversals produced interaction events in the PHA from the trapped protons. The data for the proton-induced events were collected and processed for about 7.5 active days of the 8.5-day mission

The orbit ephemeris from the STS-95 mission was used to calculate the number of predicted E>50 MeV surface incident protons per SAA traversal. Calculations were performed with NASA's AP8-MIN [6] model with its fixed magnetic field epoch of 1964 and with the new AP9 trapped proton model (V1.30.001). For the calculations with AP9, the mean model was used with the actual epoch of the mission (1998) because the new model is capable of taking into account the secular variation of the magnetic field. The predicted proton fluence per SAA traversal and the number of events measured by the PHA for orbit numbers 70-85 are plotted versus orbit number in Fig. 6 in the form of a bar chart. The figure shows that the STS-95 mission made about 15 revolutions per day around the Earth. The AP8 model predicts that 8 of the orbits traversed the SAA whereas the AP9 mean model predicts 12 SAA traversals. The sample calculations from both models predict a smooth fluence increase with a fluence of greater than 60 p/cm$^2$ and rising to a peak of about $10^6$ p/cm$^2$ at orbit numbers 75-79. After that, the proton flux smoothly decreased until there is no prediction of incident protons. This pattern repeated itself throughout the mission without significant changes due to the small daily precession of the orbit. The AP9 mean model predicts about 2 times higher proton fluences at >50 MeV for all of the STS-95 SAA passes. Also, the AP9 mean predicts that the STS-95 had 2-4 additional traversals through the SAA per day, however, most of the additional traversals were through the edges of the SAA where the traversals were less than 12 minutes in duration. The total fluence versus energy for the STS-95 7.9 day mission is plotted in Fig. 7. Note that the AP8-MIN model is for a fixed 1964 epoch for the Earth's magnetic field strength whereas the AP9 mean model uses the actual epoch of the mission. Therefore, the higher proton fluences predicted by the AP9 mean model (seen in Figures 6 and 7) are due to the shrinking strength of the Earth's magnetic field (secular variation), which brings the larger SAA region down from higher altitudes with the greater proton intensity levels. This results in longer SAA transition times and increased particle accumulation [7].

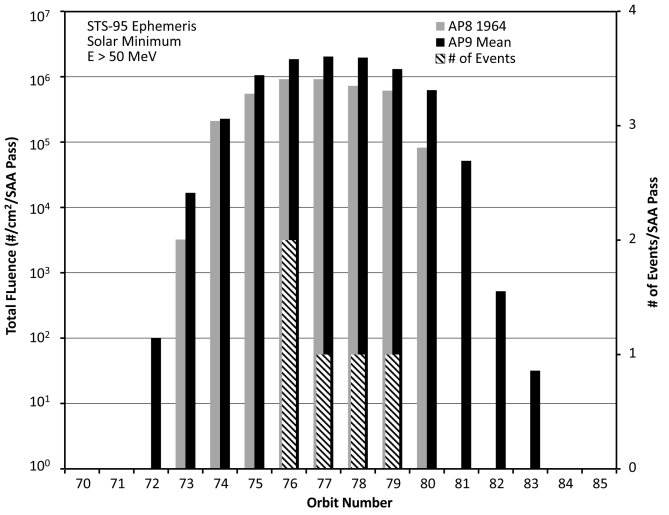


Fig. 6. Bar chart of predicted surface incident proton fluences and recorded PHA events per SAA traversal vs orbit number

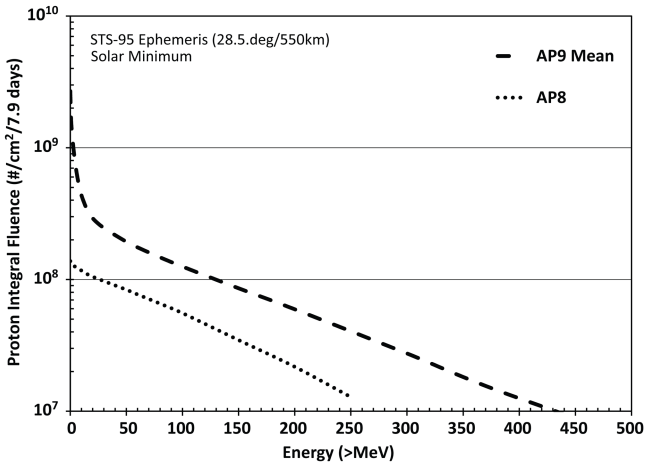


Fig. 7: Predicted surface incident proton fluences for the STS-95 Mission

Fig. 8 is a bar chart, which plots the number of STS-95 passes through the SAA according to their length of time. This provides a description of the measured traversal duration per orbit, in minutes, whether on ascending or descending nodes of the orbit. The legend distinguishes the traversals with and without the measurement of events. Statistically, the data indicate that the traversal times required for events to occur needed to exceed 13 minutes. Note from the figure that 8 of the SAA traversals that exceeded 13 minutes duration did not record any proton events. The reason for this will be discussed in Section VI.

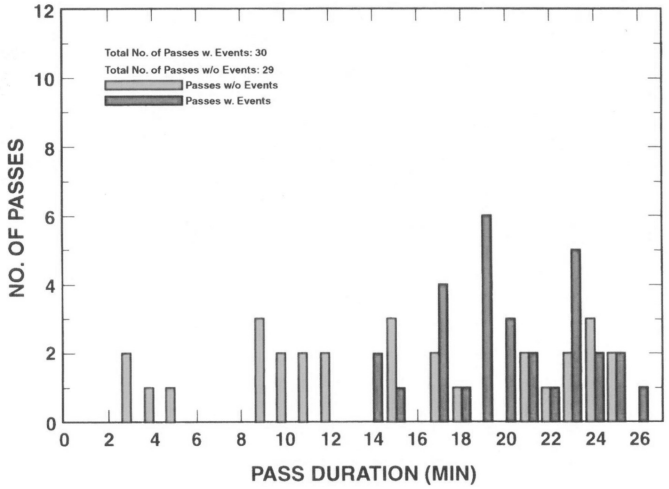


Fig. 8. Bar chart of number of SAA traversals vs. traversal duration in minutes

To further validate the PHA measurements, the SAA passes and the measurement of the events during the passes were sorted with respect to the time of occurrence. Fig. 9 shows three bar charts that illustrate the number of events and number of passes versus Greenwich Mean Time (GMT) for the 7.5-day mission. The chart on the top plots the number of events, the middle chart plots the number of SAA passes without events, and the bottom chart plots the number of SAA passes with events. It can be seen that during the time outside of the SAA, no proton-induced events were measured. This period was for GMTs from approximately hour 10 to hour 20.

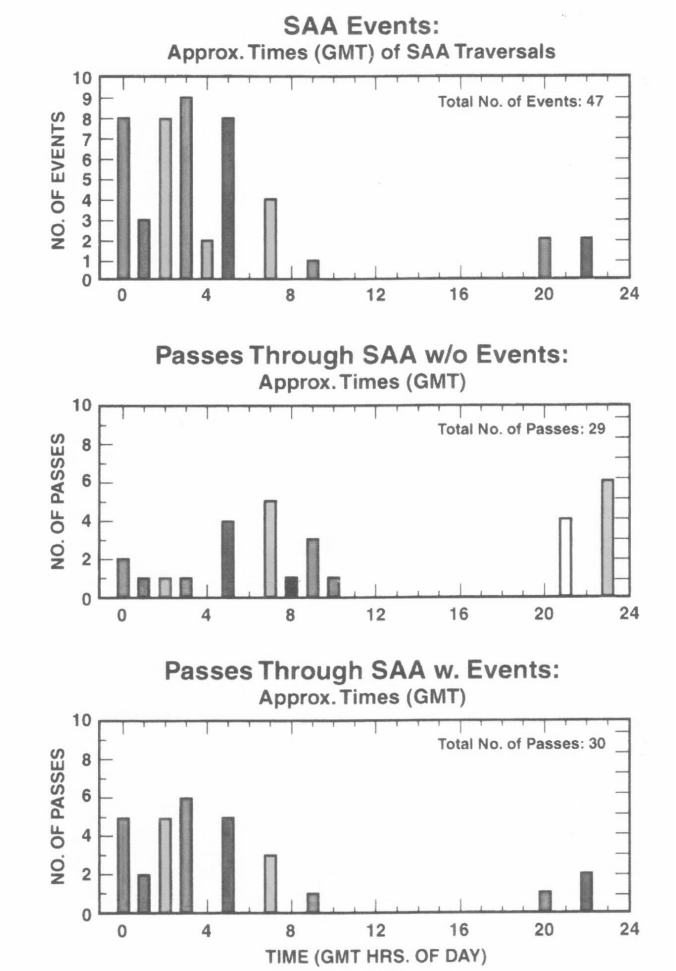


Fig. 9. Three bar-charts of SAA events and traversals vs. GMT (Greenwich Mean Time)

Fig. 10 is a geographic map at 500km altitude for latitudes from $30^0$ north to $30^0$ south. The figure displays three iso-flux contours of E > 50 MeV trapped protons for intensities of 10, 100, and 1000 particles per $cm^2/s$ for epoch 1998. The 47 proton-induced events are plotted in the geographic locations at which they were measured. It was determined that the three events located on the outermost 10-particle flux contour are valid proton-induced events and not cosmic ray induced events because, in those three locations, the predicted total number of products from proton interactions reached the critical level for triggering an event. [1]

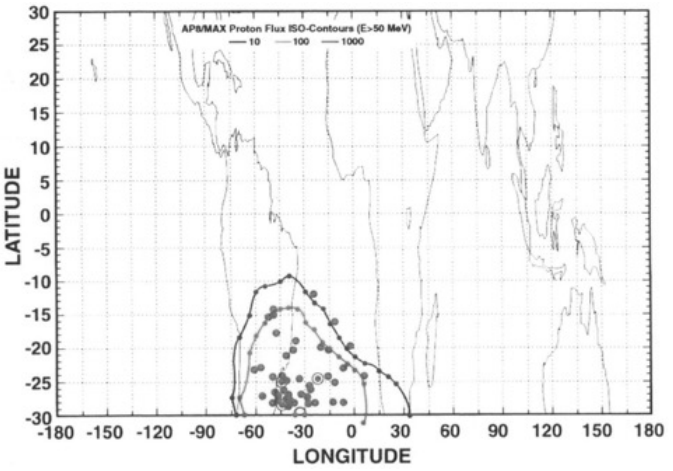


Fig. 10. Geographic map at 500 km altitude, for epoch 1998, with SAA footprint for E>50 MeV protons, showing position of proton induced events within the SAA [1]

The number of measured trapped proton induced events per channel number and their corresponding LET values are listed in Table 2. The LET values for the events in the SAA ranged from 1.12 to 1.87 MeV-cm$^2$/mg for the 47 events. All of the events occurred during the period of 7.5 days of the active time of the STS-95 mission. This yielded an average daily event rate of 6.27 events/day. A prediction of proton events for the STS-95 orbit, using the AP8-MIN model embedded in the SPENVIS code [8], yielded an event rate of 9.55 per day taking into account the detector area of 0.25 cm$^2$. Using the AP9 mean model doubles the predicted rate to about 19 events per day. This predicted rate was adjusted for the shielding and the probable low contribution of protons with energies > 200 MeV that could penetrate from the backside of the Shuttle cargo bay. This reduced the predicted event rate to 8.08 events per day using the AP8-MIN model and 16 events per day using the AP9 mean model. Although the STS-95 mission was only 7.5 days, the AP9 mean model was used because the proton fluxes at this altitude vary slowly as a function of the solar cycle.

TABLE 2
NUMBER OF PROTON EVENTS PER INSTRUMENT CHANNEL AND CORRESPONDING LET VALUES

| CHANNEL# | LET (MEV•CM$^2$/MG) | LET (KEV/µM) | NO. OF EVENTS |
|---|---|---|---|
| 12 | 1.12311 | 264 | 6 |
| 13 | 1.14940 | 270 | 2 |
| 14 | 1.17631 | 276 | 9 |
| 15 | 1.20345 | 282 | 6 |
| 16 | 1.23203 | 289 | 1 |
| 17 | 1.26087 | 296 | 4 |
| 18 | 1.29029 | 303 | 1 |
| 19 | 1.32059 | 310 | 4 |
| 20 | 1.35151 | 317 | 3 |
| 22 | 1.41553 | 332 | 5 |
| 23 | 1.44866 | 340 | 2 |
| 25 | 1.51728 | 356 | 2 |
| 27 | 1.58915 | 373 | 1 |
| 34 | 1.86859 | 439 | 1 |

*2) Galactic Cosmic Ray Induced Events*

Fig. 11 is the same geographic map used in Fig. 10, but instead of showing the proton data, it shows the location of the events that were recorded outside of the SAA. Table 3 lists the geographic latitude and longitude, the rigidity value, and the LET level for each of these 15 cosmic ray events. It is reasonable to assume that these events are induced by cosmic rays of galactic origin (GCRs) since no solar activity was reported for that interval of time.

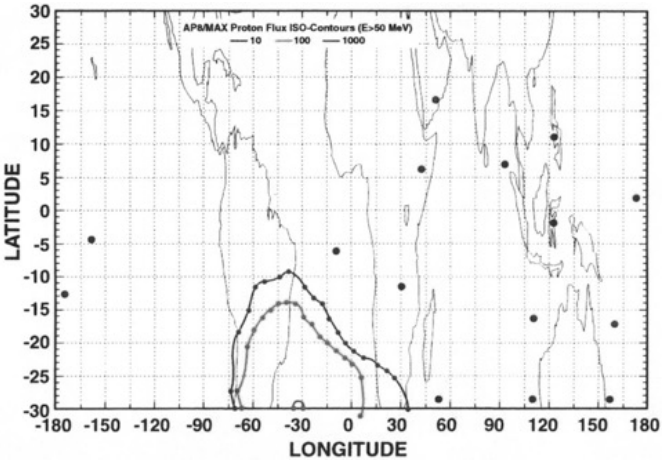


Fig. 11. Geographic map at 500 km altitude, for epoch 1998, with SAA footprint for E>50 MeV protons, showing the locations of the cosmic ray events, outside the SAA [1]

TABLE 3
COSMIC RAY EVENT RIGIDITIES, LET VALUES, AND GEOGRAPHIC POSITIONS

| LON | LAT | Cut-off Rigidity | LET (MeV•cm$^2$/mg) | LET (keV/µm) |
|---|---|---|---|---|
| 91.80 | 7.24 | 14.045 | 1.261 | 296.4 |
| 123.50 | 10.70 | 13.776 | 1.912 | 449.4 |
| 123.50 | -2.00 | 13.776 | 1.149 | 270.0 |
| 171.90 | 1.89 | 13.644 | 1.149 | 270.0 |
| 52.46 | 16.73 | 13.644 | 1.149 | 270.0 |
| 42.44 | 6.27 | 13.515 | 1.176 | 276.4 |
| -159.00 | -4.48 | 13.014 | 1.176 | 276.4 |
| -175.84 | -12.67 | 12.093 | 1.321 | 310.5 |
| 111.90 | -16.20 | 11.267 | 1.149 | 270.0 |
| -10.99 | -5.87 | 11.073 | 1.149 | 270.0 |
| 30.10 | -11.41 | 10.885 | 1.149 | 270.0 |
| 157.60 | -16.95 | 10.701 | 1.261 | 296.4 |
| 153.76 | -28.23 | 8.176 | 1.123 | 263.9 |
| 109.98 | -28.21 | 7.389 | 2.098 | 493.1 |
| 51.37 | -28.60 | 7.087 | 1.352 | 317.7 |

The LET values of the 15 events recorded outside of the SAA ranged from 1.123 to 2.098 MeV-cm$^2$/mg. It was expected that the LET values would be higher for the high-energy cosmic rays than for the protons. However, as mentioned in Section IV, it takes many protons to generate an event; therefore, the PHA is not really measuring the LET values of the actual proton particles but rather is recording the effective LET values of the proton-induced events. The 15 cosmic ray induced events were recorded over the 7.5 active mission days yielding an average rate of about 2 events per day.

All of the cosmic ray induced events occurred on or south of the magnetic equator. This is shown in Fig. 12 which outlines the SAA domain for E>50 MeV protons for the flux contour of 10 p/cm$^2$-s and the magnetic equator. The 15 cosmic ray events recorded over the 7.5 active mission days

are plotted at the geographic location where they were measured. A probable reason for this will be discussed in Section VI. [1]

This map also shows the magnetic L-shell parameter contours [9] of values from approximately 1.05 to 10.0 Earth radii, corresponding to rigidities R (in MV) of 14.9 to 6.2, respectively, obtained from the IGRF-1995 magnetic field model at the 500 km altitude level for epoch 1998. The energies that are necessary for cosmic rays to penetrate the magnetosphere to reach these locations range from approximately 1.15 GeV/n to about 5.6 GeV/n as discussed above.

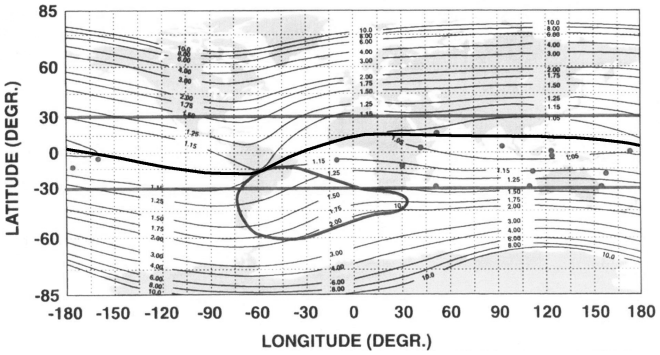


Fig. 12. Geographic map at 500 km altitude, for epoch 1998, with SAA footprint for E>50 MeV protons, showing position of cosmic ray induced events outside the SAA

## VI. Discussion of Results

The purpose of this section is to provide understanding of why 8 of the traversals through the SAA, which exceeded 13 minutes duration did not produce events measured by the PHA and to understand why the cosmic ray induced events were located south of the magnetic equator.

### *A. Trapped Proton Induced Events*

Previous studies have shown that the intensity of the trapped proton and cosmic ray particles incident on the spectrometer likely varied with the attitude (orientation) of the STS-95 vehicle during its traversals through the SAA [10]. To illustrate this, a software program, "Satellite Tool Kit" (STK), developed by Analytic Graphics Inc. [11], was used to visualize the attitude of the STS-95 vehicle during its presence in the SAA. For example, Fig. 13 shows the attitude of the vehicle in a 0,0,0 configuration with the x-axis parallel to the shuttle velocity vector while the z-axis points to the center of the Earth, and Fig. 14 shows the position of the shuttle with an attitude of 45,45,45. The line crossing the shuttle represents the Shuttle trajectory going from the left to the right.

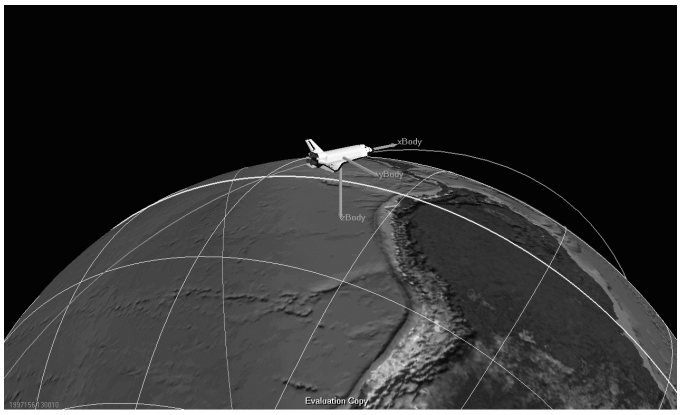


Fig. 13. View of the shuttle body axis at 0,0,0, x-axis parallel to the shuttle velocity vector, z-axis pointing to the center of the Earth

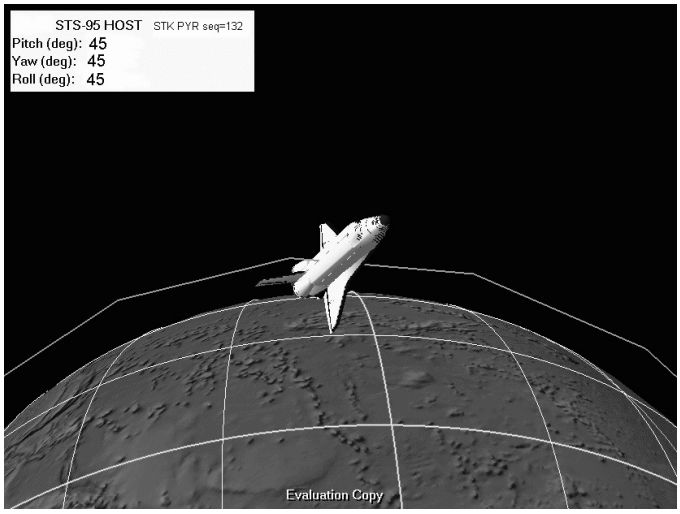


Fig. 14. Position of the shuttle with an attitude of 45,45,45

Fig. 15 shows a traversal of the SAA when the bay of the Shuttle is oriented to west-north-west. In this case, the main constituent of the flux has to cross only the bay to reach the detector. On the other hand, Fig. 16 shows that, during some traversals through high intensity regions of the SAA, the Shuttle was oriented such that protons had to pass through significant shielding, therefore, could not reach the detector to produce an event. Note that one STK generated image showed that the Shuttle grazed the SAA contour but the event occurred at a high channel number, that is, at a high LET value, and thus it was classified as a cosmic ray generated event rather than a proton event.

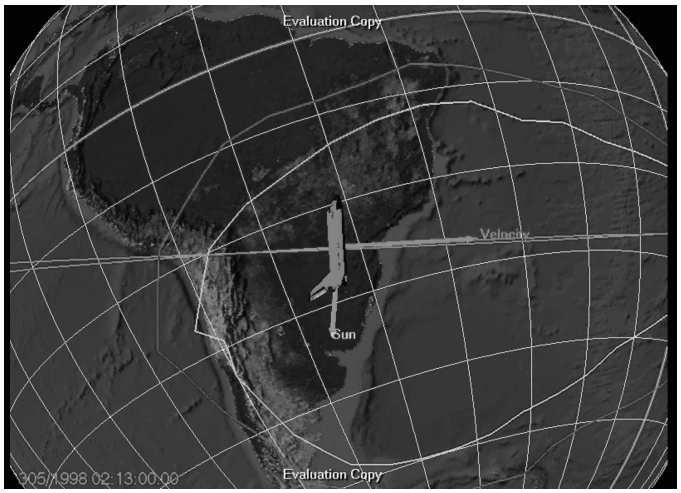

Fig. 15. Position of the Shuttle inside the SAA when an event occurred

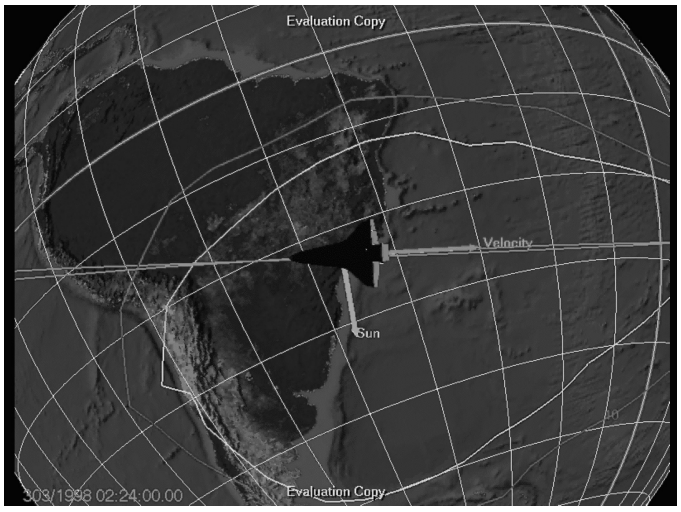

Fig. 16. Position of the shuttle inside the SAA without event.

Fig. 17 is a plot similar to Fig. 6 showing the predicted proton fluence per SAA traversal and the number of events measured by the PHA for orbit numbers 55-70. Note that, although SAA passes 60 and 62 resulted in PHA events, no events were recorded for pass 61. Examination of the STS-95 ephemeris file shows that the Shuttle was performing maneuvers during passes 60-62, temporarily placing the Shuttle in an orientation such that the cargo bay was heavily shielded during pass 61. It is concluded that the orientation of the Shuttle as it passed through the SAA explains why the PHA did not measure events in 8 of the SAA traversals that were greater than 13 minutes in duration (see Fig. 8). This also partially explains why the predicted event rate was higher than the measured event rate.

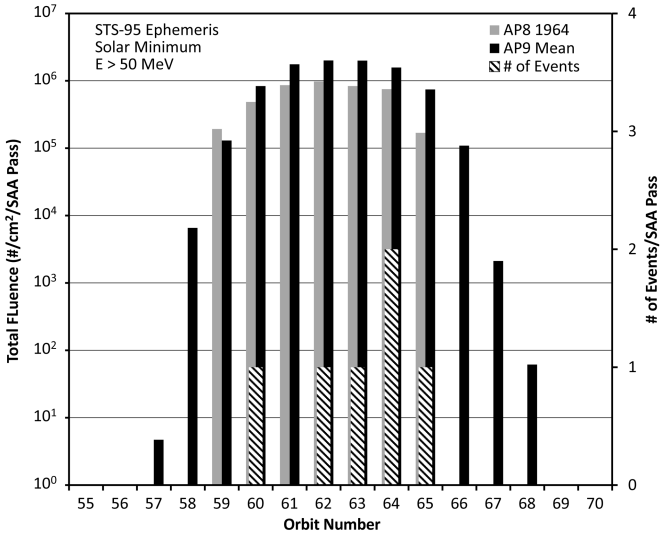

Fig. 17. Bar chart of predicted surface incident proton fluences and recorded PHA events per SAA traversal vs orbit number

The impact of the Shuttle orientation is magnified when considering the East-West proton flux anisotropy at the Shuttle altitude of 550km. This anisotropy is due to particles moving westward with their centers of gyration below the Shuttle, experiencing more interactions with the atmosphere than those moving eastward which have their centers of gyration above the Shuttle. Particles from below are only those that survived their mirror point location without falling into the atmospheric cutoff domain at about 100-200 km altitude. The cutoff altitude varies depending on the significant changes that occur with time in the atmospheric density. These atmospheric density temporal variations are believed to reach up to a factor of 200 between the maximum and minimum periods of solar activity. In addition, diurnal variations in the atmospheric density are estimated to reach a factor of 10.

It is difficult to assess the degree of proton anisotropy for this mission because the Shuttle does not fly in a fixed orientation, and the mission duration was short. The Compact Environment Sensor (CEASE) on the Tri-Service Experiment-5 satellite measured the degree of anisotropy for ~40 MeV protons from 2000-2006 [12]. At 600 km altitude, the measured ratio of the East/West proton flux was about 2. The ICARE-NG/CARMEN-1 (Influence sur les Composants Avancés des Radiations de l'Espace-Nouvelle Génération/CARactérisatin et Modélisation de l'Environnement spatial) detector on board the low Earth orbit Argentinean SAC-D satellite measured the degree of anisotropy from 2011-2012 [13]. Those measurements showed that at 700 km altitude the anisotropy for 29 MeV protons could be up to a factor of 10. For this work, we assumed an East/West ratio of 2.7 for 100 MeV protons based on measurements from the STS-94 mission [14,15].

The 47 proton induced events are listed in Table 4 which contains (a) the daily time (in minutes) spent by the shuttle in the SAA region for the seven full days, (b) the time in the SAA with events, (c) the time in the SAA without events, and (d) the total time in the SAA, and the respective number of passes. The daily average visitation time is about 138 minutes.

The LET range of these particles extended from about 1.2 to about 1.9 MeV-cm$^2$/mg. It can be concluded that the difference of about 20% in the measured proton event rate to the predicted rate is due to the effects of the shuttle's orientation during passes through the SAA and the narrow angle of incidence of the spectrometer's detector.

TABLE 4
DAILY TIME SPENT BY THE SHUTTLE IN THE SAA, WITH AND WITHOUT EVENTS AT 28.5°/550 KM

| DAY OF YEAR | TIME IN SAA W EVENTS (MIN) | TIME IN SAA W/O EVENTS (MIN) | TOTAL TIME IN SAA (MIN) |
|---|---|---|---|
| 303 | 50 | 91 | 141 |
| 304 | 88 | 50 | 138 |
| 305 | 101 | 34 | 135 |
| 306 | 89 | 46 | 135 |
| 307 | 71 | 71 | 142 |
| 308 | 102 | 37 | 139 |
| 309 | 45 | 88 | 133 |
| DAYS 303-309 | 546 | 417 | 963 |
| | W EVENTS (#) | W/O EVENTS (#) | TOTAL (#) |
| PASSES | 30 | 29 | 59 |
| EVENTS | 47 | 0 | 47 |

### *B. Galactic Cosmic Rays*

As discussed in Section V, the cosmic ray events were concentrated south of the magnetic equator (seen in Fig. 12). An analysis of the Shuttle position and attitude [10] showed that the Shuttle orientation had no influence on the galactic cosmic ray induced events. A possible explanation is the prevailing Interplanetary Magnetic Field (IMF) direction when aligned in the north direction [16] as shown in Fig. 18. This anisotropy arises from the gyro-orbits of the cosmic ray particles about the IMF.

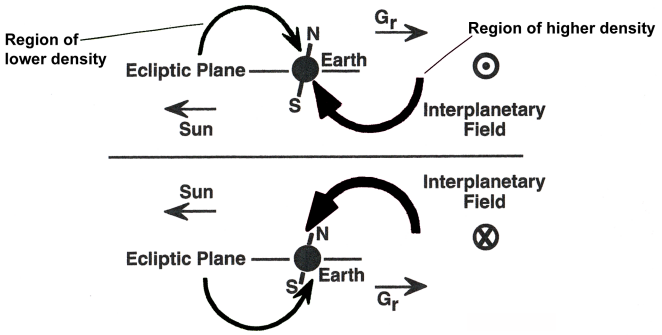


Fig. 18. Cosmic ray N-S anisotrophy and dependence on the IMF direction [1]

Further, Fig. 19 is a plot of differential flux (#/cm$^2$-day-MeV/n) of Si ion cosmic rays, versus energy (MeV/n), for low earth orbits (LEO) at an altitude of 600 km, in terms of magnetospherically unattenuated and attenuated intensities for circular orbits at three inclinations: 90˚, 57˚, and 28˚. These data clearly indicate the significant shielding provided by the Earth's magnetic field, which effectively deflects the cosmic ray heavy ions through the rigidity effect (particle momentum over charge). The figure shows that the effect is pronounced for low inclination orbits.

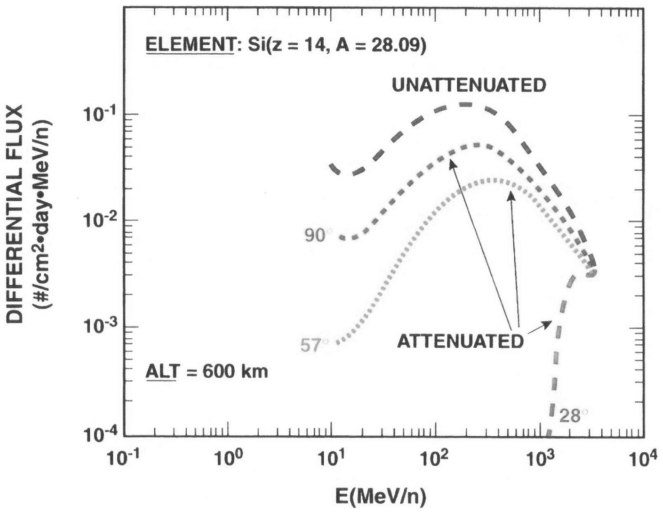


Fig. 19. Attenuation of Si cosmic ray ions by the Earth's magnetic field for LEO orbits

## VII. CONCLUSIONS

The measurements of the HOST PHA spectrometer are in close agreement with the predictions of trapped proton induced events in the SAA. Based on PHA calibrations, estimates were calculated with the SPENVIS code using NASA's AP8-MIN proton model for solar minimum conditions and the new AP9 mean model. The predictions were about two times higher using the AP9 model. The PHA measurements also showed the effect of the shrinking Earth's magnetic field on the location of the SAA and on the intensity of the protons trapped there.

The rate of measured events indicate that under quiet solar and magnetospheric conditions, missions in low-inclination (<35$^0$) and low-altitude (<1000 km) orbits experience the lowest exposure to trapped and transiting space radiation, providing maximum possible natural protection for biological and electronic systems. These results from the STS-95 mission also clearly demonstrate that the low power, small size, and lightweight PHA is an effective proton and heavy ion monitor for space programs as it effectively measures *in situ* particles. Such measurements are particularly valuable for understanding the cause of spacecraft anomalies and failures.

## VIII. ACKNOWLEDGEMENTS

The authors wish to thank Martha O'Bryan for her outstanding editorial and graphics support.

## REFERENCES

[1] E. G. Stassinopoulos, J. L. Barth, and C. A. Stauffer, "Measurement of Cosmic Ray and Trapped Proton LET Spectra on the STS-95 HOST Mission," *in Proc. RADECS*, Bremen Germany, 2016, to be published.

[2] G. P. Ginet, T. P. O'Brien, S. L. Huston, W. R. Johnston, T. B. Guild, R. Friedel, C. D. Lindstrom, C. J. Roth, P. Whelan, R. A. Quinn, D. Madden, S. Morley and Yi-Jiun Su, "AE9, AP9 and SPM: New Models for Specifying the Trapped Energetic Particle and Space Plasma Environment," *Space Sci Rev*, vol. 179, no. 1, pp. 579–615, Mar. 2013.

[3] E. G. Stassinopoulos, C. A. Stauffer, and G. J. Brucker, “Miniature high-LET radiation spectrometer for space and avionics applications,” *Nucl Instrum Methods Phys Res A*, vol. 416, no. 2-3, pp. 531-535, Nov. 1998.
[4] P. J. McNulty, D. R. Roth, W. J. Beauvais, W. G. Abdel-Kader, and E. G. Stassinopoulos, “Microdosimetry in Space Using Microelectronic Circuits,” *Proc in NATO ASI Series A: Life Sciences*, vol. 243B, Algarve, Portugal, 1991, pp. 165-178.
[5] D. R. Roth, P. J. McNulty, W. J. Beauvais, R. E. Reed, A. V. Thompson, and E. G. Stassinopoulos, “Solid State Microdosimeter for Spacecraft Applications,” *in Proc. RADECS*, Saint Malo, France, 1993, pp. 84-87.
[6] D. Sawyer, and J. Vette, “AP8 trapped proton environment for solar maximum and minimum,” *National Space Science Data Center*, Greenbelt, Maryland, Rep. *76-06*, 1976.
[7] E. G. Stassinopoulos, M. A. Xapsos, and C. A. Stauffer. (2016, Dec.). Forty-Year “Drift” and Change of the SAA. NASA Goddard Space Flight Center. Greenbelt, MD. [Online]. Available: http://ntrs.nasa.gov/archive/nasa/casi.ntrs.nasa.gov/20160003393.pdf
[8] SPENVIS: The Space Environment Information System. Belgian Institute for Space Aeronomy. Brussels, Belgium. [Online]. Available: http://www.spenvis.oma.be/
[9] C. E. McIlwain, “Coordinates for mapping the distribution of magnetically trapped particles,” *Geophys Res*, vol. 66, no. 11, pp. 3681–3691, Nov. 1961.
[10] A. Guillet, E. G. Stassinopoulos, C. A. Stauffer, M. Dumas, J-M. Palau, and M-C. Calvet, *“Study of Vehicle Attitude Effect on Shuttle Radiation Measurements,”* NASA Goddard Space Flight Center, Greenbelt, MD, Rep. *NASA/TM-2001-209995*, 2001.
[11] Satellite Tool Kit, distributed by Analytical Graphics, Inc., 325 Technology Drive, Malvern, PA 19355 USA.
[12] G. P. Ginet, B. K. Dichter, D. H. Brautigam, and D. Madden, “Proton Flux Anisotropy in Low Earth Orbit,” *Trans on Nucl Sci*, vol. 54, no. 6, pp. 1975-1980, Dec. 2007.
[13] D. Boscher, T. Cayton, V. Maget, S. Bourdarie, D. Lazaro, T. Baldran, P. Bourdoux, E. Lorfevre, G. Rolland, and R. Ecoffet, "In-Flight Measurements of Radiation Environment on Board the Argentinean Satellite SAC-D," *Trans on Nucl Sci*, vol. 61, no. 6, pp. 3395-3400, Dec. 2014.
[14] H. D. R. Evans, and E. J. Daly, “Anisotropies in the Low Altitude Radiation Environment,” *British Interplanetary Society Journal*, vol. 48, no. 3, pp. 149-157, Mar. 1995.
[15] G. D. Badhwar, V. V. Kushin, Yu. A. Akatov, and V. A. Myltseva, “Effects of Trapped Proton Flux Anisotropy on Dose Rates in Low Earth Orbit,” *Radiat Meas*, vol. 30, no. 3, pp. 415-26, Jun. 1999.
[16] M. L. Duldig, “Australian Cosmic Ray Modulation Research,” *Electronic Pubs of the Astronomical Society of Australia*, vol. 18, no. 1, Apr. 2001. [Online]. Available: http://www.atnf.csiro.au/pasa/18_1/index.html